JOURNAL OF MATERIALS SCIENCE 24 (1989) 281–287

Pearlite spheroidization

Ö. E. ATASOY
Faculty of Technical Education, Gazi University, Ankara, Turkey
S. ÖZBILEN*
The Middle East Technical University, Ankara, Turkey

The static spheroidization of a silicon-containing steel was studied employing quantitative metallography and hardness measurements. Specimens with interlamellar spacings of 0.57 and 0.26 μm were annealed at temperatures of 600, 650 and 700° C to obtain the spheroidization of Fe_3C. The results of quantitative metallography and hardness measurements indicate that the rate of spheroidization is controlled by the diffusion of iron at the Fe–Fe_3C interface. The increase in the rate of spheroidization due to a reduction in the interlamellar spacing is thought to be caused by an increase in the defect density in the Fe_3C plates when pearlite has a smaller interlamellar spacing.

1. Introduction

It is a fact that the process of spheroidization of lamellar structures, both in the case of pearlite of steels and in that of eutectic structures, has been the subject of various studies. Some of these studies [1–3] were devoted to the structural developments during spheroidization with quantitative metallography techniques being used to assess their extent. Other studies reported the results of work on the increasing rate of spheroidization by cold-working prior to annealing or by concurrent deformation [1, 3–5]. The apparent effect of the magnitude of the interlamellar spacing was also studied [2, 6] and it was discovered that the rate of spheroidization increases when the interlamellar spacing decreases.

The mechanisms proposed [2, 7, 8] for the static spheroidization process involve pinching off at faults in the internal structure of the discontinuous phase. With regard to the rate-determining step in the case of static spheroidization, the general trend was towards a bulk diffusion control mechanism [1, 9]. Another work [6] was based on measuring the mean curvature of the average ferrite–cementite interface at temperatures of 650 and 700° C, the authors finding an activation energy comparable to iron diffusion at the ferrite–cementite interface.

The present work reports the results of spheroidization experiments carried out at three temperatures: 600, 650 and 700° C, on a silicon-containing eutectoid steel.

2. Experimental procedure

The material used in the present work was taken from an ingot cast in the Department of Metallurgy of the Middle East Technical University, Ankara, and had the composition 0.59% C, 0.69% Mn, 1.19% Si, 0.022% P and 0.061% S. A cylinder 6 cm dia. × 4.5 cm long was prepared from the material and was cut into two equal parts lengthwise. The two identical pieces of material thus obtained were then austenitized at 850° C. Following this process, one of the pieces was air-cooled while the other piece was furnace-cooled, in order to obtain two separate pieces with two different interlamellar spacings. Finally, one specimen was cut from each heat-treated piece and approximately 30 random test-lines were drawn on the SEM micrographs of these two specimens and used to measure their mean interlamellar spacings. It was discovered that the air-cooled specimen had a mean interlamellar spacing value of 0.26 μm, while the furnace-cooled specimen had a 0.57 μm mean interlamellar spacing.

Further specimens with dimensions of 1 cm × 1 cm × 0.4 cm were annealed in a non-airtight furnace for varying times up to 2200 h at temperatures of 600, 650 and 700° C and it was discovered that a scale formed which was reasonably well attached to the surface (Fig. 1). On the other hand, however, a gap between the scale and the material beneath was observed on the surface of some of the specimens which had been subjected to long annealing times. X-ray diffraction work carried out on the oxidized surface of the specimens indicated the presence of Fe_2O_3 and Fe_3O_4 oxides with no wustite (FeO) formation. Similar results had been reported previously [10], that is, if the carbon is in a combined form, the scale is made up of a haematite and magnetite in equal amounts when the material is subjected to long annealing times at temperatures below the eutectoid temperature. In this work, on those specimens having an oxidized surface there was no sign of any decarburized layer near the oxide scale. This fact was also confirmed by chemical analysis of the carbon content of the above-mentioned specimens, and this analysis showed that there had been no carbon loss to the furnace atmosphere from the specimens during annealing.

* *Present address*: Department of Materials Science, Queen Mary College, London, E1 4NS, UK.

0022–2461/89 $03.00 + .12

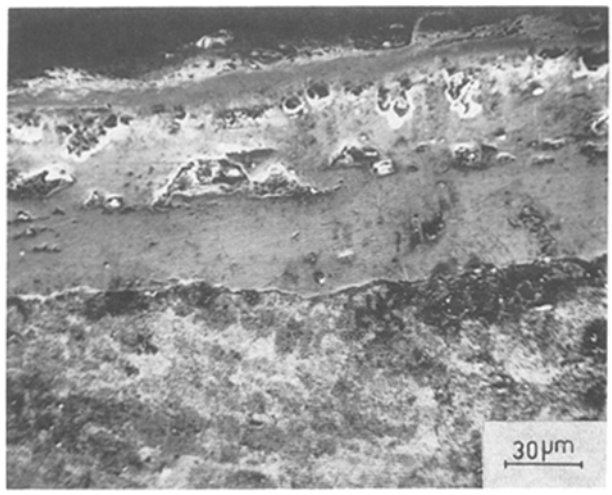

Figure 1 The oxide scale formed on specimens annealed for long times.

With the exception of a number of trials using transmission electron microscopy, scanning electron microscopy was used for the greater part of the work in order to study the starting structure and to follow up the progress of spheroidization. The starting materials had a pearlitic structure (Fig. 2), even though the carbon content was lower than that of the eutectoid composition of a pure Fe–C alloy. The shift of the eutectoid composition in the present material was due to the presence of silicon and manganese, and the combined effects of both these elements gave a eutectoid composition of 0.57% C for the present material [11]. In addition, the effect of silicon and manganese on the eutectoid temperature was calculated and it was noticed that the eutectoid temperature of the material was 729° C. Therefore, the 700° C temperature chosen as the highest working temperature for the present work was well below the eutectoid temperature of the present steel.

3. Results

The initial materials had a pearlitic structure with pearlite colony sizes of about 10 and 5 μm for the furnace-cooled and normalized materials, respectively. The aspect ratios of the cementite plates were measured on SEM micrographs and in each specimens the dimensions of about 1000 particles were measured. The aspect ratio values calculated from these measurements were first divided into class intervals and then plotted against their relative frequencies. An example of this is given in Fig. 3. The aspect ratio values of the starting materials ranged from 1 : 1 to 34 : 1 for the normalized material and from 1 : 1 to 45 : 1 for the furnace-cooled material. The criterion of an aspect ratio value of 8 : 1 was adopted to determine the percentage spheroidization, and the area of the spheroidized and unspheroidized particles was calculated by adopting the methods used by Chattopadhyay and Sellars [2] who assumed the spheroidized particles to

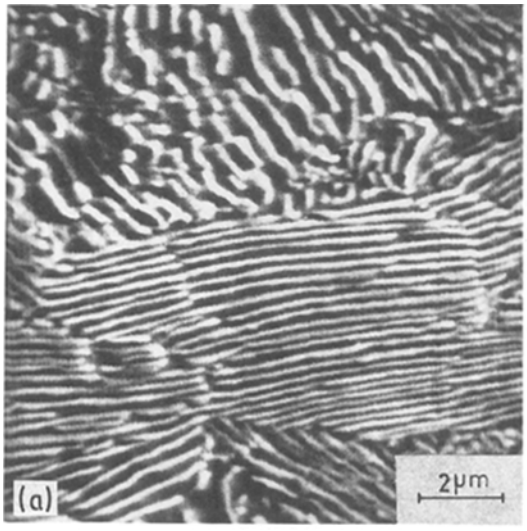

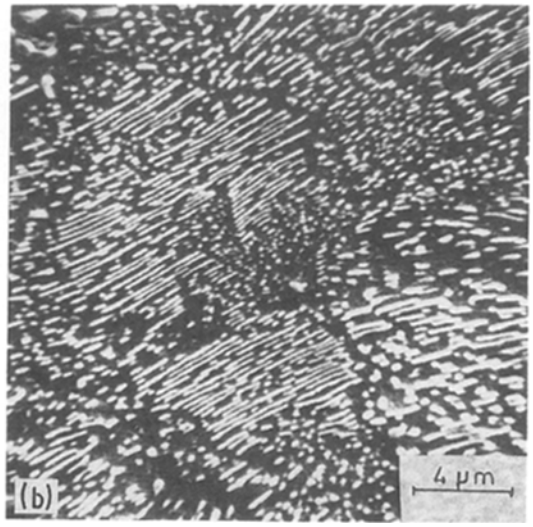

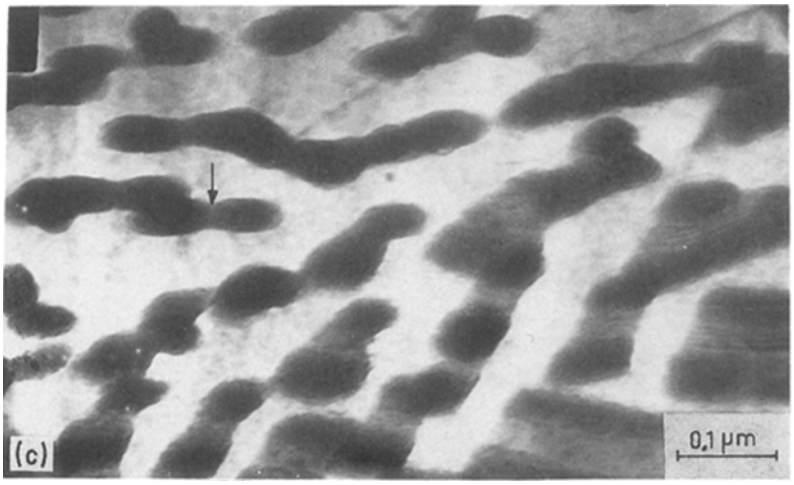

Figure 2 SEM micrographs of (a) normalized material and (b) the same material after about 58% spheroidized; (c) TEM micrograph of normalized material. Arrow shows one of the triple-point junctions.

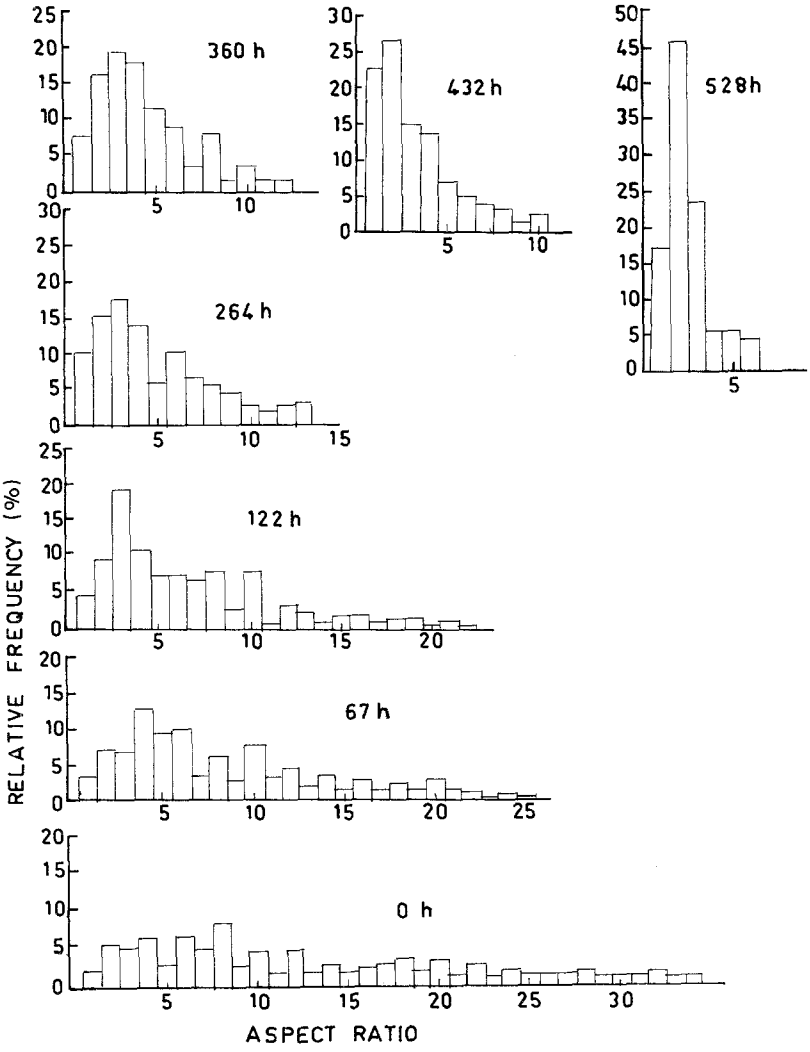

Figure 3 Aspect ratio measurements at 700° C for furnace-cooled material. Interlamellar spacing is 0.57 μm.

be ellipses and the unspheroidized ones to be rectangles. The following equation was used to calculate the percentage spheroidization for each specimen:

$$F = \frac{V_s}{V_c} \times 100$$

where $V_s = \Sigma N_s S_s$ = the volume fraction of the spheroidized particles, $V_c = V_s + V_u$ = the volume fraction of the cementite particles and $V_u = \Sigma N_u S_u$ = the volume fraction of the unspheroidized particles; S_s and S_u are the areas of the spheroidized and unspheroidized particles while N_s and N_u are their numbers per unit area, respectively.

The hardness of the specimens was measured on a Knoop hardness tester using a 500 g load. The hardness values, after conversion to VPN, of the furnace-cooled material before the spheroidization anneal and in the 100% spheroidized state were 2090 and 1650 MPa, respectively, while the normalized material had hardness values of 2450 and 1770 MPa under the

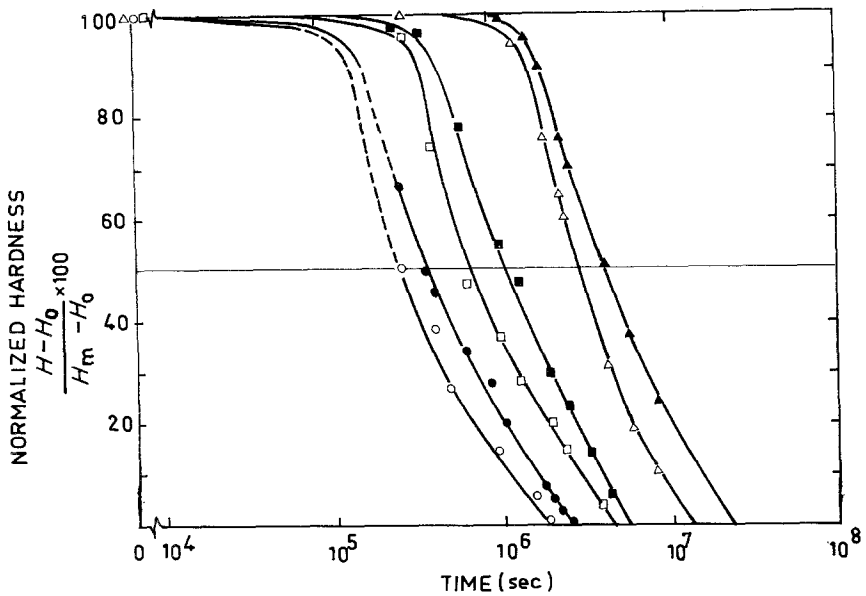

Figure 4 Change in normalized hardness with time. Interlamellar spacing 0.57 μm: (▲) 600° C, (■) 650° C, (●) 700° C. Interlamellar spacing 0.26 μm: (△) 600° C, (□) 650° C, (○) 700° C.

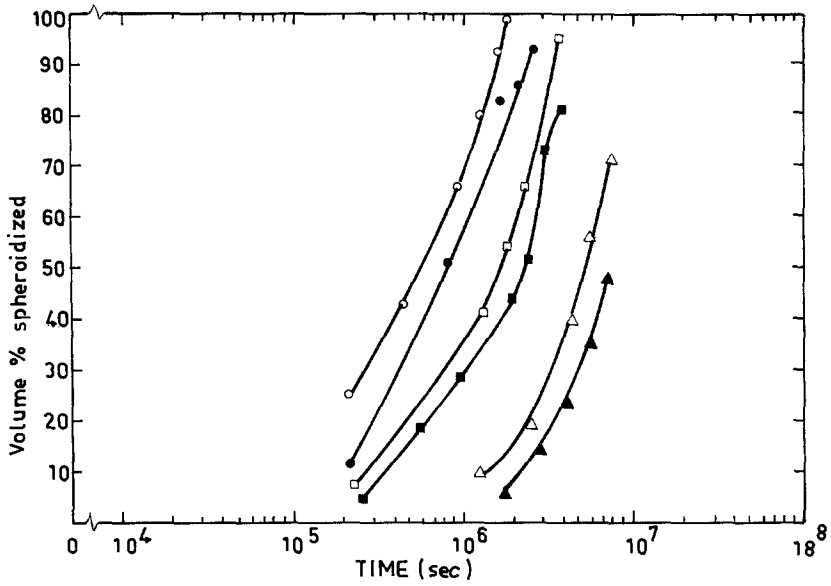

Figure 5 The change in spheroidization percentage with time. Interlamellar spacing 0.57 μm: (▲) 600° C, (■) 650° C, (●) 700° C. Interlamellar spacing 0.26 μm: (△) 600° C, (□) 650° C, (○) 700° C.

same conditions. The hardness values of the specimens with varying degrees of spheroidization were measured and are plotted in Fig. 4, after the hardness values had been normalized according to the expression

$$\text{Normalized hardness} = \frac{H - H_0}{H_m - H_0}$$

where H_m = hardness of the material before the onset of spheroidization, H_0 = hardness of the material after 100% spheroidization is achieved and H = hardness of a specimen after annealing for a certain time which had aquired a certain amount of spheroidization.

The change in hardness with time (Fig. 4) is closely related to the progress of spheroidization, (Fig. 5). An incubation time was necessary for the hardness values to start to decrease and this time corresponded to that of the start of spheroidization. The normalized hardness values of the partially spheroidized specimens were the same for the same amount of spheroidization irrespective of other process variables. Such a result is not surprising, since hardness values are related to the microstructure of a material. Both Figs 4 and 5 also indicate that the rate of spheroidization increases with decreasing interlamellar spacing.

4. Discussion

The structural developments which took place during the spheroidization annealing of the present work confirm the idea of Lupton and Warrington [3] that pinching off of the Fe_3C plates through the migration of triple junctions, such as those shown on the TEM micrograph of Fig. 2c, is partly responsible for spheroidization. It was also possible to observe discontinuities on a set of Fe_3C plates with their terminations falling on nearly straight lines on the micrographs of the starting material (Fig. 2), and these observations were similar to the observations on some eutectic structures [12]. Such regular terminations were observed to increase with annealing and it was assumed that these terminations occurred on internal faults in Fe_3C plates. These faults were possibly formed during the formation of pearlite, although the reason for their formation is not known.

The progress of spheroidization obtained from the aspect ratio measurements showed that spheroidization proceeds faster with increasing temperature and

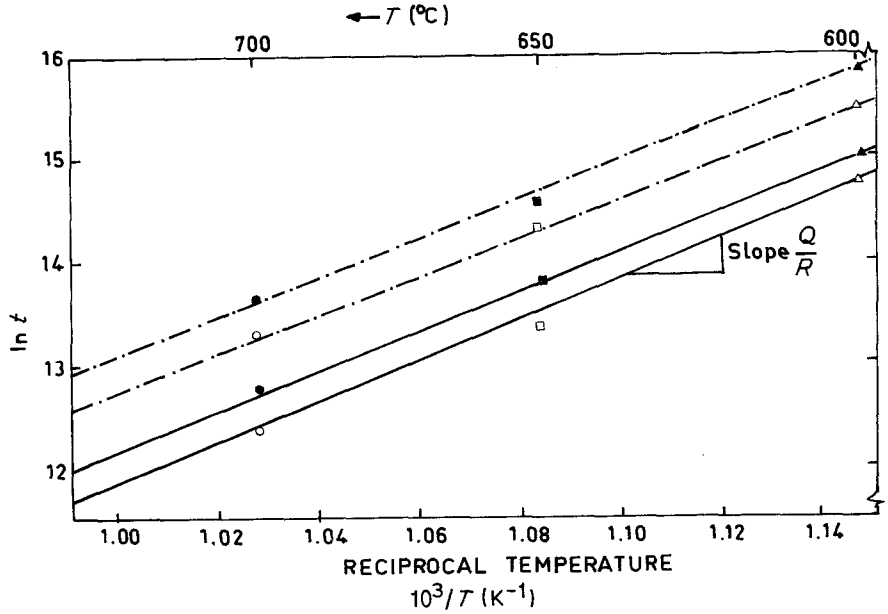

Figure 6 Variation of times for (—·—) 50% spheroidization (F = 0.5) and (——) half reduction in normalized hardness (NH = 0.5) with the reciprocal of absolute temperature. Interlamellar spacing 0.57 μm: (▲) 600° C, (■) 650° C, (●) 700° C. Interlamellar spacing 0.26 μm: (△) 600° C, (□) 650° C, (○) 700° C.

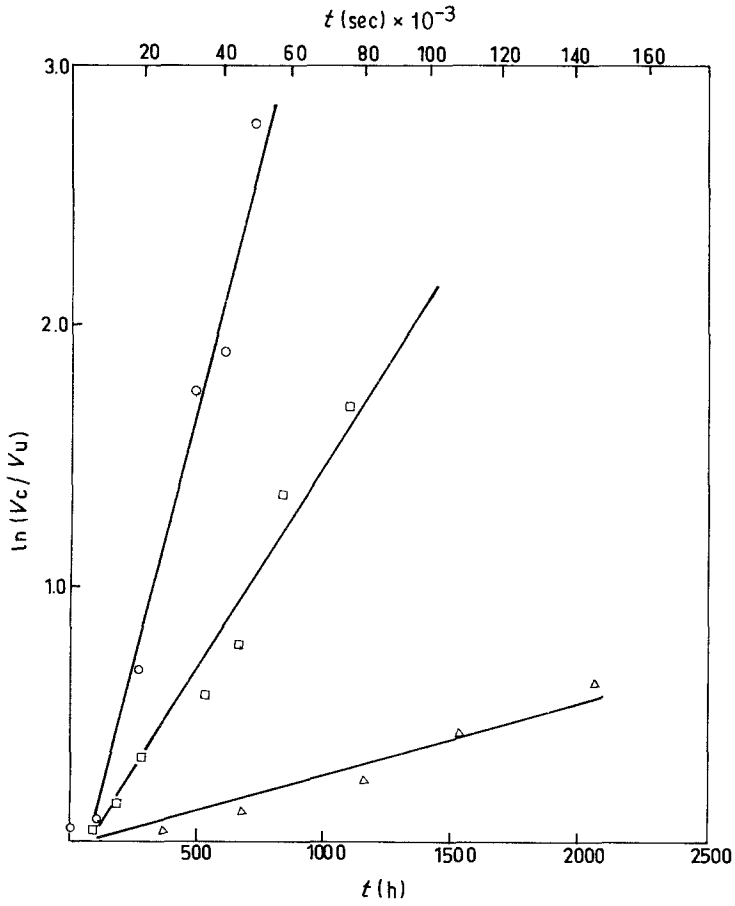

Figure 7 Ratio of total carbide volume/unspheroidized carbide volume against time for furnace-cooled material ($S = 0.57\,\mu m$): (△) 600° C, (□) 650° C, (○) 700° C.

decreasing interlamellar spacing (Fig. 5). The latter effect was reported previously; however, it was not possible to detect the presence of any peak formation at specific aspect ratio values on the histograms (Fig. 3), contrary to a previous work [2].

It is also clear from Figs 4 and 5 that hardness change follows the progress of spheroidization. The results of the development of spheroidization with time (Fig. 5) and the change in normalized hardness can both be used to obtain the activation energy for spheroidization. The time necessary for 50% spheroidization and the time which should elapse for the normalized hardness to drop by half were found from Figs 4 and 5 and are plotted in Fig. 6 against the reciprocal of temperature. The activation energy values calculated by using the 50% spheroidization time were 159 and 160 kJ mol^{-1} for normalized and furnace-cooled materials, respectively. On the other hand, the use of normalized hardness values gave 179 and 175 kJ mol^{-1} for the same materials. These values are close to those for grain boundary diffusion of iron atoms in iron [13], thereby suggesting that iron diffusion along the Fe–Fe_3C interface is the controlling mechanism for static spheroidization in carbon steels.

In the Appendix, the volume fraction of the spheroidized particles, V_s, is calculated as a function of time (Equation A7) as

$$V_s = V_c [1 - A \exp(-C\bar{a}x^2 t)]$$

By substitution of $V_s = V_c - V_u$ in the above equation, and by rearranging the said equation, the following is obtained:

$$\frac{V_c}{V_u} = \frac{1}{A} \exp(C\bar{a}x^2 t)$$

In the final equation, we may substitute $C\bar{a}x^2 = k$, where k is the spheroidization rate. The k values can be obtained from Fig. 7, which shows the change in ln (V_c/V_u) with time. The k values obtained in this way can be used to obtain the activation energy values, if the k values are plotted against the reciprocal of the absolute temperature. In this way, the values 181 and 156 kJ mol^{-1} were calculated as the activation energy for the spheroidization of the furnace-cooled and normalized materials, respectively. These results again confirm that the interface diffusion of iron at the iron–cementite interface is the controlling mechanism for static spheroidization.

As was mentioned above, the reduction in interlamellar spacing increases the rate of spheroidization. Chattopadhyay and Sellars [2] reported that when the interlamellar spacing was increased by a factor of 6.5, the time for 50% spheroidization increased by a factor of 1.75 at 700° C. In the present work, however, it was found that when the interlamellar spacing was increased by a factor of 2.2, the time for 50% spheroidization increased by a factor of 1.46, which is the average of the increments obtained at three spheroidization temperatures, i.e. 600, 650 and 700° C. On the other hand, for the same change in interlamellar spacing, the ratio of k values averaged for the above-mentioned temperatures was about 1.15.

The results of the present work and those of Chattopadhyay and Sellars [2] are thought not to be in contradiction with the argument that the process of spheroidization is controlled by interface diffusion. At first sight it might be expected that when the interlamellar spacing is increased by a certain factor the rate of spheroidization would decrease by the same

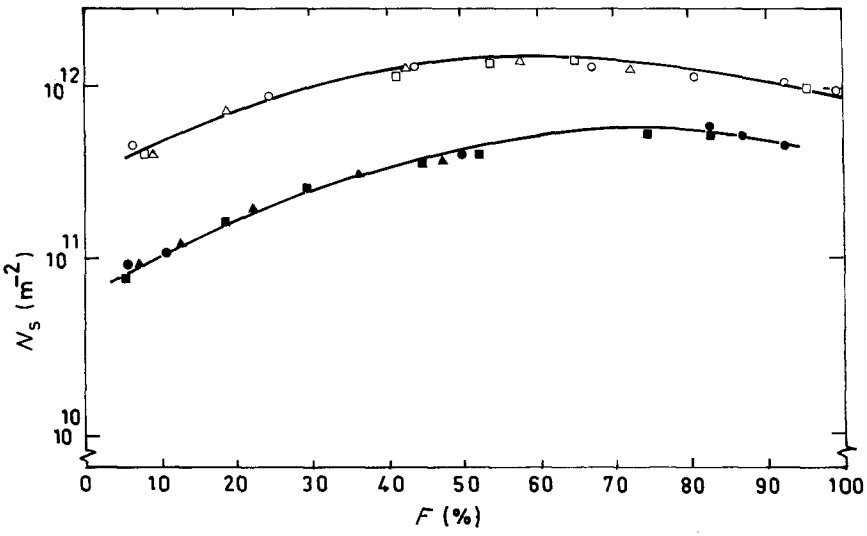

Figure 8 Change in the number of particles spheroidized, N_s, with percentage spheroidization, F. Interlamellar spacing 0.57 μm: (▲) 600° C, (■) 650° C, (●) 700° C. Interlamellar spacing 0.26 μm: (△) 600° C, (□) 650° C, (○) 700° C.

factor, since such an increase in interlamellar spacing should decrease the number of plates per unit area as well as the number of Fe–Fe_3C interfaces. As a result, the cross-section of the area where diffusion takes place should also be reduced. Such an argument would be correct if any change in interlamellar spacing, which is accomplished by transforming austenite at different temperatures, does not affect the internal structure of the Fe_3C plates. We are inclined to believe that the number of defects in the Fe_3C plates increases with the reduction in interlamellar spacing as a result of a reduction in the transformation temperature. In other words, the term C defined in the Appendix will assume different values when the interlamellar spacing is changed. During the examination of specimens in the SEM, it was often possible to observe quite different amounts of spheroidization in the neighbouring pearlite grains. This non-uniformity is thought to result from the difference in density of the structural inhomogenieties in the Fe_3C plates in different grains.

The number of spheroidized particles, N_s, should have increased with time continuously if no particle coarsening had been taking place. On the other hand, the experimental results indicate that in Fig. 8, N_s first increases with time and then starts to decrease after passing through maxima which correspond to the 60 and 70% spheroidization values for the normalized and furnace-cooled materials. The decrease in the rate of increase of N_s with the increase in percentage spheroidization is due to the decrease in unspheroidized volume. However, the existence of the maxima in Fig. 8 is due to particle coarsening. These maximum values in Fig. 8 correspond to the time when the rate of formation of new particles due to spheroidization is equal to the rate of disappearance of the already spheroidized particles through coarsening in localized areas.

Appendix

Let us borrow the following two equations from Chattopadhyay and Sellars [2]:

$$V_s + V_u = V_c \tag{A1}$$

$$\frac{dV_s}{dt} = \frac{dN_s}{dt} a\bar{x}^2 \tag{A2}$$

where V_s and V_u are the spheroidized and unspheroidized volume fractions, respectively, N_s is the number of spheroidized particles per unit area, a is the aspect ratio and $\bar{x}$ is the mean thickness of the unspheroidized particles.

Since the spheroidization of lamellar structures requires the pinching-off of the lamellae, let us define a parameter C, the rate of pinching-off of plates with aspect ratio a per unit time per unspheroidized unit area, C is thought to be a function of the number of defects in the plates and the atomic diffusion. We can then write the equation

$$\frac{dN_s}{dt} = CV_u \tag{A3}$$

Let us combine Equations A3 and A2:

$$\frac{dV_s}{dt} = CV_u a\bar{x}^2 \tag{A4}$$

Since V_c = constant,

$$\frac{dV_s}{dt} = \frac{dV_u}{dt}$$

Then

$$\frac{dV_u}{dt} = -CV_u a\bar{x}^2 \tag{A5}$$

Integration of Equation A5 gives

$$V_u = AV_c \exp(-Ca\bar{x}^2 t) \tag{A6}$$

where A is the integration constant and $A \leqslant 1$ depends on the spheroidized volume fraction at $t = 0$.

Substitution $V_u = V_c - V_s$ in Equation A6. After rearranging,

$$V_s = V_c[1 - A \exp(-Ca\bar{x}^2 t)] \tag{A7}$$

It follows that the number of spheroidized plates, i.e. N_s, if no coarsening was taking place, can be calculated after dividing V_s by $a\bar{x}^2$:

$$N_s = \frac{V_c}{a\bar{x}^2}[1 - A \exp(-Ca\bar{x}^2 t)] \tag{A8}$$

References

1. E. A. CHOJNOWSKI and W. J. McG. TEGGART, *Metal. Sci. J.* **2** (1968) 14.

2. S. CHATTOPADHYAY and C. M. SELLARS, *Metallography* **10** (1977) 89.
3. D. F. LUPTON and D. H. WARRINGTON, *Metal. Sci. J.* **6** (1972) 200.
4. H. PAQEUTON and A. PINEAU, *J. Iron Steel Inst.* **209** (1971) 991.
5. J. L. ROBBINS, O. C. SHEPPARD and O. D. SHERBY, *ibid.* **202** (1964) 604.
6. A. K. GOGIA and A. M. GOKHALE, *Met. Trans.* **11A** (1980) 1077.
7. F. A. NICHOLS and W. W. MULLINS, *Trans. Met. Soc. AIME* **233** (1965) 1840.
8. R. RACEK and G. Le SOULT, *J. Crystal Growth* **16** (1972) 223.
9. E. HO and G. C. WEATHERLY, *Metal Sci. J.* **7** (1977) 141.
10. D. CAPLAN, G. I. SPROWE, R. J. HUSSEY and M. J. GRAHAM, *Oxid. Metals* **13** (1979) 255.
11. E. C. BAIN and H. W. PAXTON, "Alloying Elements in Steel", 2nd Edn (American Society for Metals, Ohio, 1961).
12. L. D. GRAHAM and R. W. KRAFT, *Trans. AIME* **236** (1966) 94.
13. E. JAMES and P. LEAK, *Phil. Mag.* **12** (1965) 491.

Received 4 March 1986
and accepted 18 May 1988